Supporting Information for

Heteroatom coordination induces electric field polarization of single Pt sites to promote hydrogen evolution activity

Xianyun Peng,[†,a] Haihong Bao,[†,a] Jiaqiang Sun,[b] Zhiyong Mao,*[,c] Yuan Qiu,[a] Zhaojun Mo,*[,d] Longchao Zhuo,[e] Shusheng Zhang,[f] Jun Luo,[a] and Xijun Liu*[a,g]

[a]   Institute for New Energy Materials and Low-Carbon Technologies and Tianjin Key Lab for Photoelectric

       Materials & Devices, School of Materials Science and Engineering, Tianjin University of Technology,

       Tianjin 300384, China. E-mail: xjliu@tjut.edu.cn (X. J. Liu)

[b]   State Key Laboratory of Coal Conversion, Institute of Coal Chemistry, Chinese Academy of Sciences,

       Taiyuan 030001, Shanxi, China.

[c]   School of Materials Science and Engineering, Tianjin University of Technology, Tianjin 300384, China.

       E-mail: mzhy1984@163.com (Z. Y. Mao)

[d]   Ganjiang Innovation Academy, Chinese Academy of Sciences, Jiangxi 341000, China. E-mail:

       mozhaojun@gia.cas.cn (Z. J. Mo)

[e]   School of Materials Science and Engineering, Xi'an University of Technology, Xi'an 710048, China.

[f]   College of Chemistry, Zhengzhou University, Zhengzhou 450000, China.

[g]   Key Laboratory of Civil Aviation Thermal Hazards Prevention and Emergency Response, Civil Aviation

       University of China, Tianjin 300300, China.

† Authors contributed equally to this work.

Experimental section

Synthesis of Pt-SA/MXene

MXene was prepared according to our previous work (Small 2020, 16, 2002888). The Pt-SA/MXene catalyst could be easily obtained via ultrasonizing the mixture solution of MXene and Pt precursor. In typically, 200 µL of 6 mg ml^{-1} freshly prepared chloroplatinic acid solution was added to 100 ml MXene suspension solution (1 mg ml^{-1}) solution. The mixture was vigorously ultrasonicated for 1 h under a flowing Ar atmosphere in an ice bath to minimize oxidation. After that, Pt-SA/MXene was obtained by centrifuging and freeze-drying.

Synthesis of Pt-NP/MXene

For the synthesis of Pt-NP/MXene, 500 µL of 6 mg ml^{-1} freshly prepared chloroplatinic acid solution was adding into 100 ml of MXene suspension solution (1 mg ml^{-1}) with electromagnetic stirring for 30 min. Then, 24 mg of sodium borohydride was quickly added into the above resultant mixture under vigorous stirring for 2 h at 0 °C using an ice bath to maintain the temperature for the prevention of Pt nanoparticle aggregations. Subsequently, the resulting solution was centrifuged and washed with deionized water. Finally, the Pt-NP/MXene composite was obtained by freeze-drying.

Materials characterization

X-ray diffraction (XRD) was conducted with an X-ray diffractometer (Rigaku SmartLab 9 kW) with Cu Kα radiation (λ = 0.154598 nm) at a scan rate of 10° min^{-1} from 3° to 70°. The morphology and elemental composition were carried out by transmission electron microscopy (TEM) and energy-dispersive X-ray spectroscopy (EDX) mappings using FEI Talos F200X instruments. Atomic-resolution high-angle annular dark-field scanning transmission electron microscopy (HAADF-STEM) images were obtained by using a Titan Themis 60-300 STEM equipment equipped with a spherical probe aberration corrector. X-ray photoelectron spectrometry (XPS) characterizations were performed on the Thermo Scientific Al Kα XPS system

(ESCALAB250Xi), and the binding energies were calibrated by setting the measured binding energy of C 1s, 284.8 eV. ICP-OES analysis was conducted on a Thermo iCAP RQ instrument. The elemental analysis was performed by an elemental analyzer (Vario EL cube).

XAFS measurements

XAFS spectra were obtained at the 1W1B station in BSRF (Beijing Synchrotron Radiation Facility, China) operating at 2.5 GeV with a maximum current of 250 mA. XAFS measurements at the Pt L_3-edge were performed in the fluorescence mode using a Lytle detector. Athena and Artemis codes were used to extract data and fit profiles.

XAFS data analysis

The acquired EXAFS data were processed with the ATHENA package software. The k^3-weighted χ (k) data in the k-space ranging from 3.0 to 11.0 Å^{-1} were Fourier-transformed to real (R) space to separate the EXAFS contributions from different coordination shells. The EXAFS data fitting in the R range of (1.1, 3.0) Å was carried out by using the ARTEMIS software. The structural parameters of bond distance (R), coordination numbers (N), and the Debye-Waller factor (σ^2) were treated adjustable during the fitting process.

Electrochemical tests

Electrochemical measurements were performed with an electrochemical workstation (CHI 760C, CH Instruments Inc.) in 1 M KOH aqueous solution using a three-electrode configuration. An Ag/AgCl electrode and carbon rod were used as the reference and counter electrode, respectively. The catalyst ink was prepared by mixing 6 mg of catalyst powder, 0.5 mL of Nafion (0.05 wt.%) solution, and 0.5 mL of absolute ethyl alcohol. The mixed solution was sonicated for 1 h to form homogeneous catalytic ink. Then, the working electrode was prepared by dropping 20 μL of the catalyst ink on the glassy carbon electrode. HER polarization curves were achieved at a potential sweep rate of 10 mV s^{-1}. The electrochemical double-layer

capacitance was probed by cyclic voltammetry (CV) at non-faradaic potentials as another way to reckon the efficient electrochemical active area of HER. Current-time responses were monitored by chronoamperometric measurements for 27 h.

Computational details

All the DFT calculations were performed using the VASP package with VASPKIT code for post-processing the calculated data. Generalized gradient approximation (GGA) with the Perdew-Burke-Ernzerhof (PBE) functional is employed to treat the exchange-correlation energy. The interaction between core and valence electrons was described by the projected augmented wave (PAW) basis set. A converged cutoff was set to 400 eV. In geometry optimizations, the force convergence standard was set below 0.01 eV Å^{-1}. The 3 × 3 × 1 Monkhorst–Pack k-point mesh was used for each Pt-SA/MXene and Pt (111) slab optimization. The bottom two layers were fixed to implement the free energy calculation of each intermediate. A 15 Å vacuum layer was constructed along the z-axis for each model. Contributions of zero-point energies (ZPE), enthalpy, and entropy were considered and calculated. The calculation details of the Gibbs free energy change (ΔG) were expressed as follows:

$$\Delta G = \Delta E + \Delta E_{ZPE} + \int C_p dT - T\Delta S$$

where ΔE is the electronic energy difference between the free-standing and the adsorption states of the intermediates; $\int C_p dT$ is the enthalpic temperature correction. ΔE_{ZPE} and ΔS is the corrections of zero-point energy and variation of entropy, respectively.
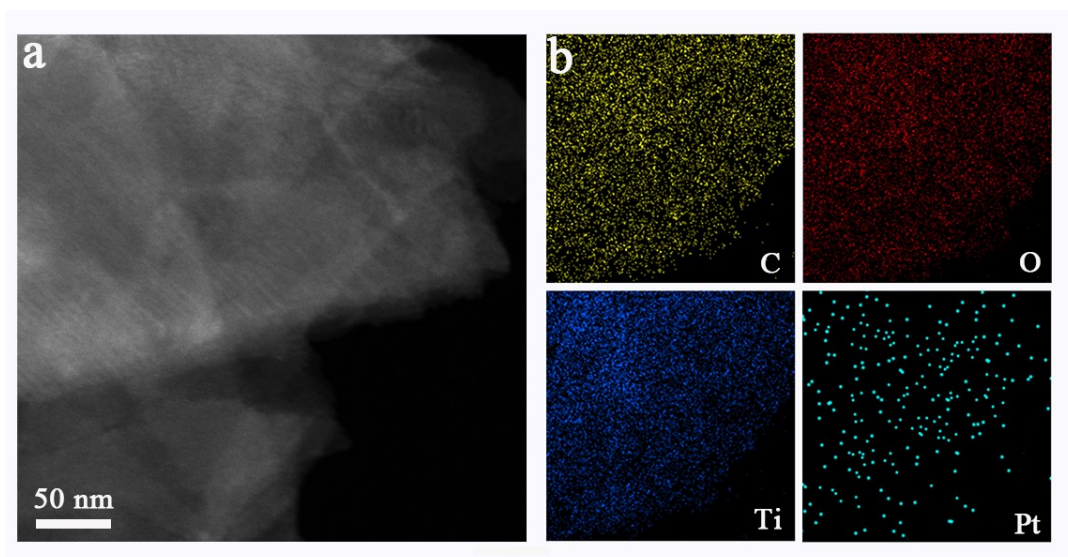
Figure S1. The EDX elemental mappings of Pt-SA/MXene. (a) HAADF-STEM image. (b) The EDX elemental mapping images.
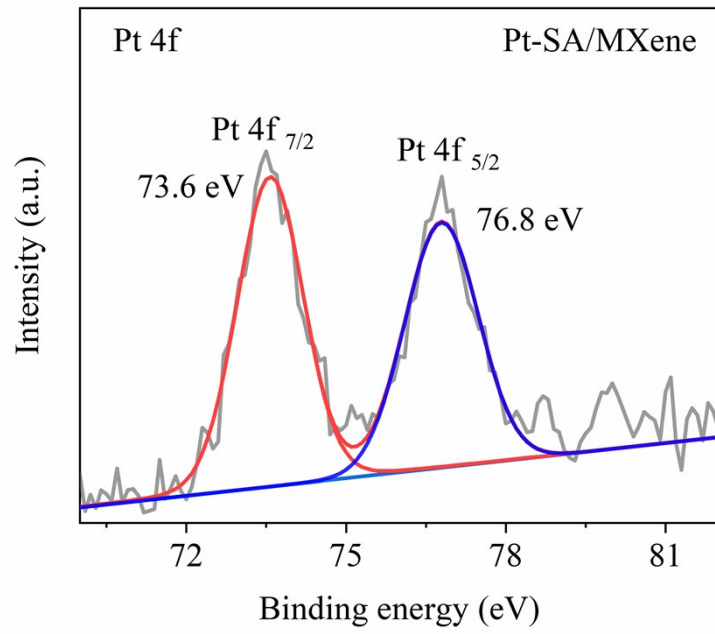
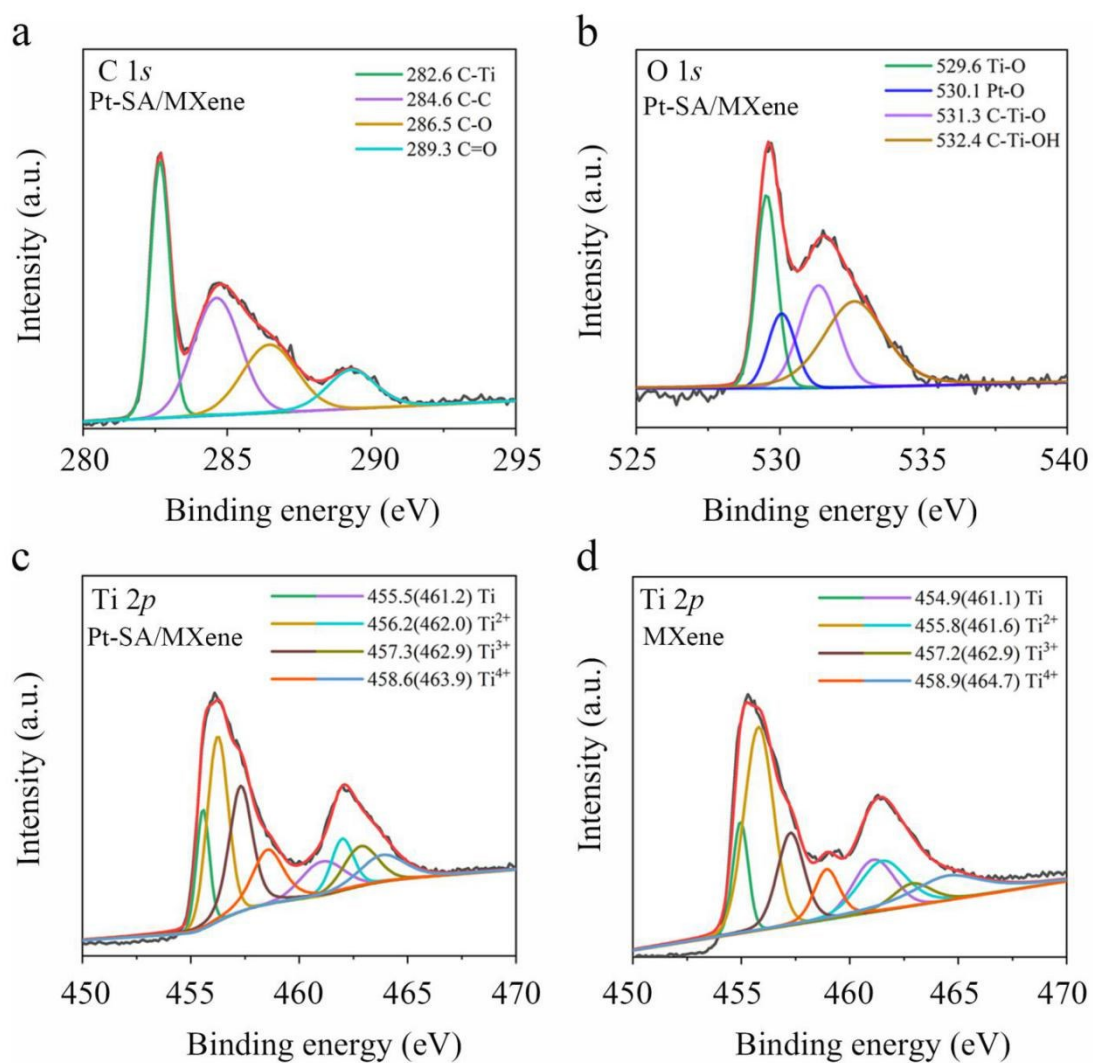**Figure S2.** High-resolution XPS of Pt 4f in the Pt-SA/MXene sample.

Figure S3. XPS results of Pt-SA/MXene and MXene. (a-C) C 1s, O 1s and Ti 2p spectra of Pt-SA/MXene, (d)Ti 2p spectra of MXene.
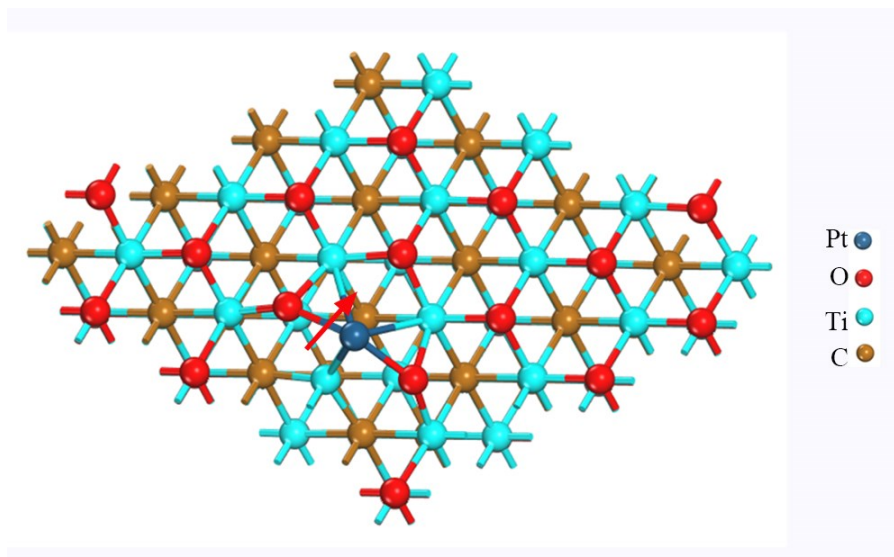
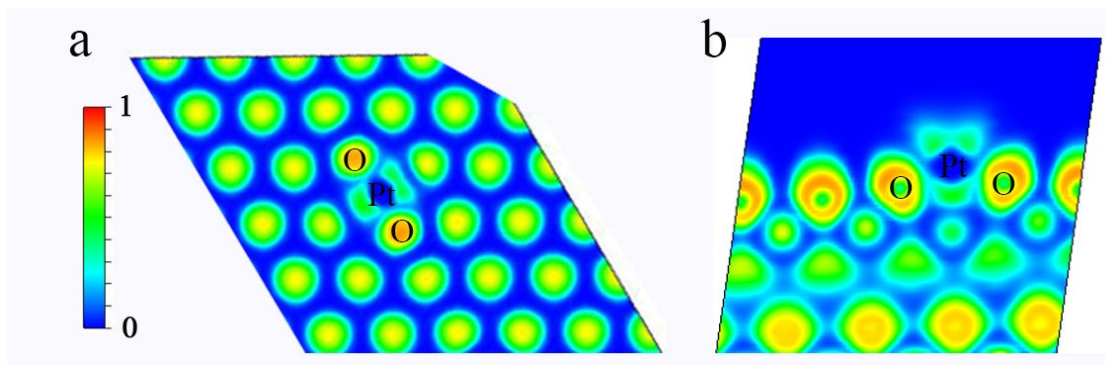**Figure S4.** The top-view atomic structure of the Pt-SA/MXene sample.

Figure S5. Electron localization function the Pt-SA/MXene sample (a) top view and (b) side view.
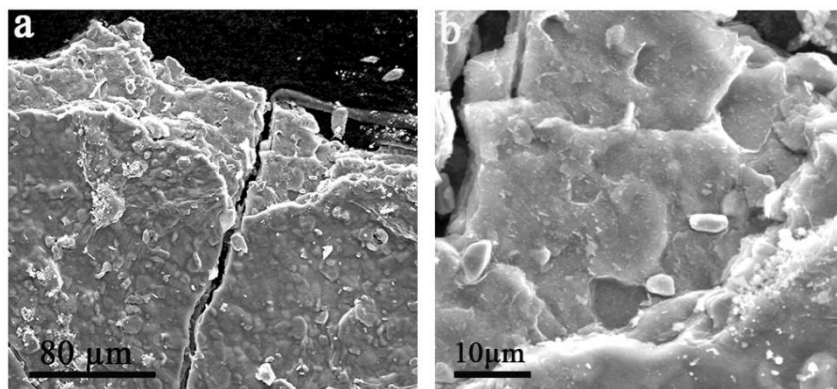
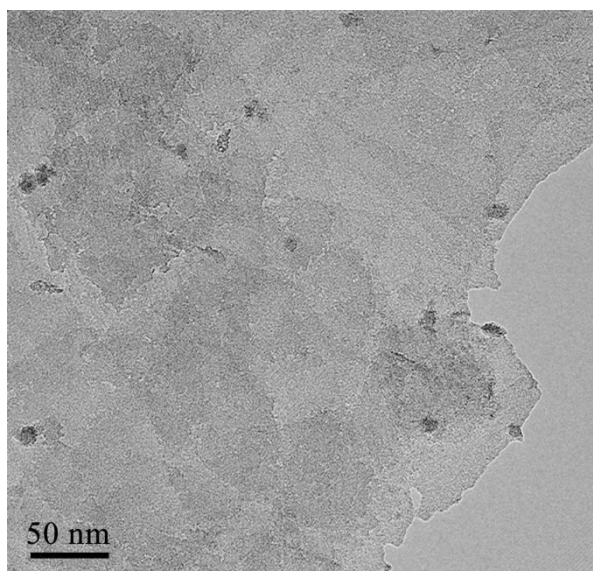**Figure S6.** The SEM image of the Pt-NP/MXene sample.

Figure S7. The TEM image of the Pt-NP/MXene sample. The Pt nanoparticles are uniformly dispersed on ultrathin MXene nanosheets.
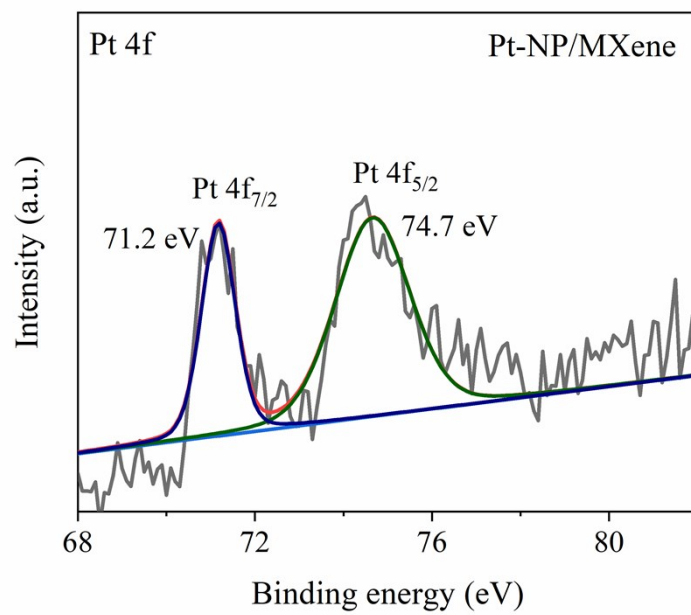
Figure S8. The High-resolution XPS of Pt 4f in the Pt-NP/MXene sample. The Pt 4f peaks at 71.2eV and 74.7

eV indicate the Pt^0 valence value state of Pt in the Pt-NP/MXene sample.[20]
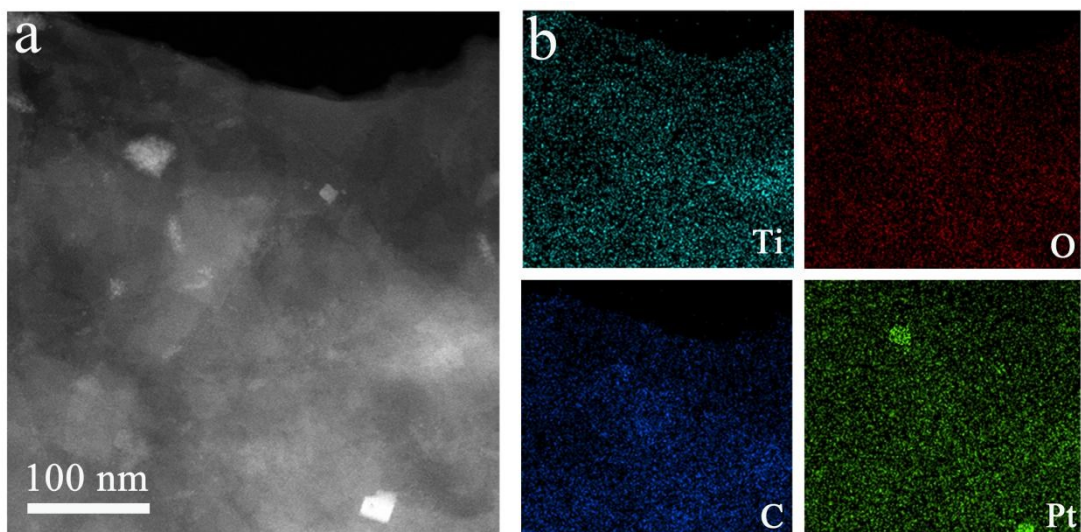
Figure S9. The EDX elemental mappings of Pt-NP/MXene. (a) HAADF-STEM image. (b) The EDX elemental

mapping images. It indicated the appearance of Pt nanoparticles and the homogeneous dispersion of the
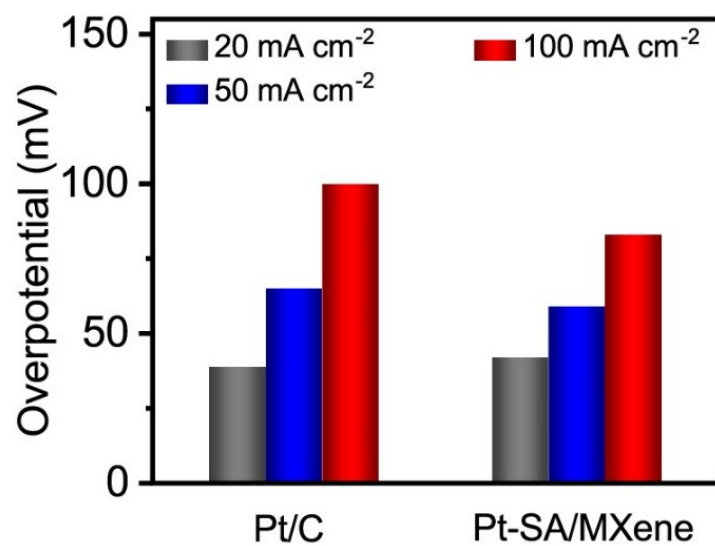
Ti, C, and O elements.

Figure S10. The overpotential comparison diagram of Pt-SA/MXene and Pt/C at different current densities.
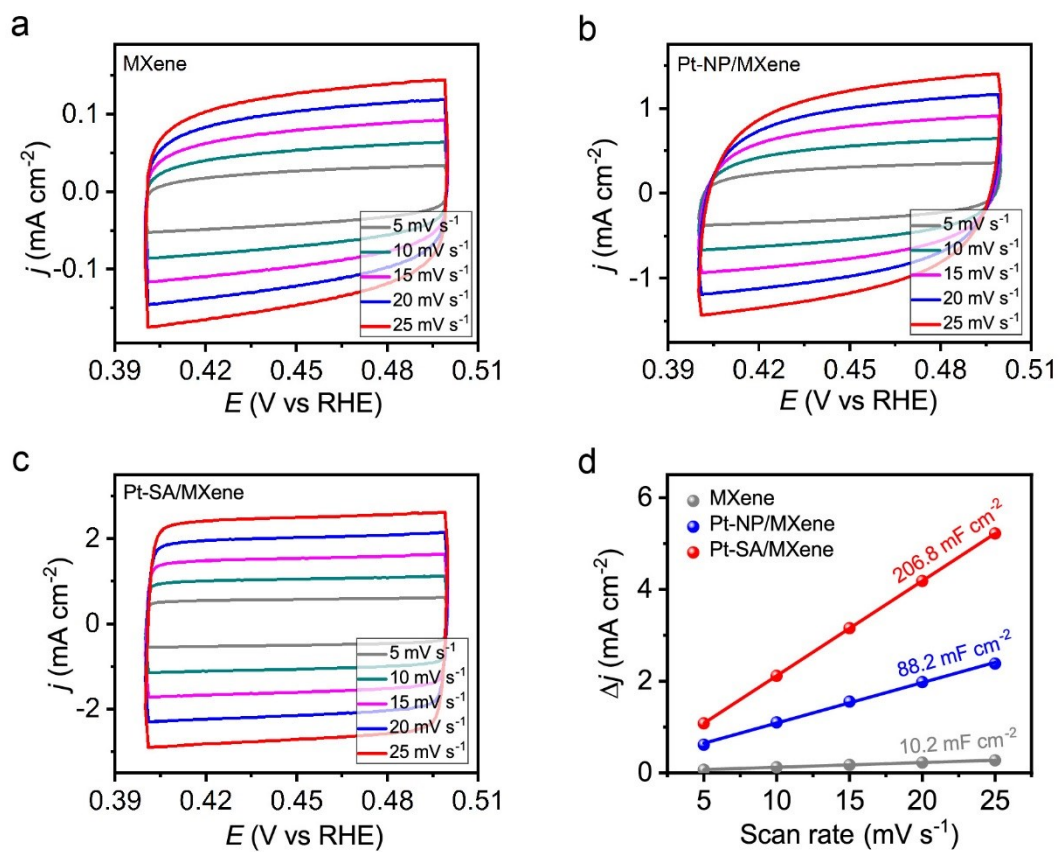
Figure S11. The cyclic voltammograms of (a) MXene, (b) Pt-NP/MXene, and (c) Pt-SA/MXene electrodes with various scan rates. (d) The capacitance current densities as a function of scan rate.
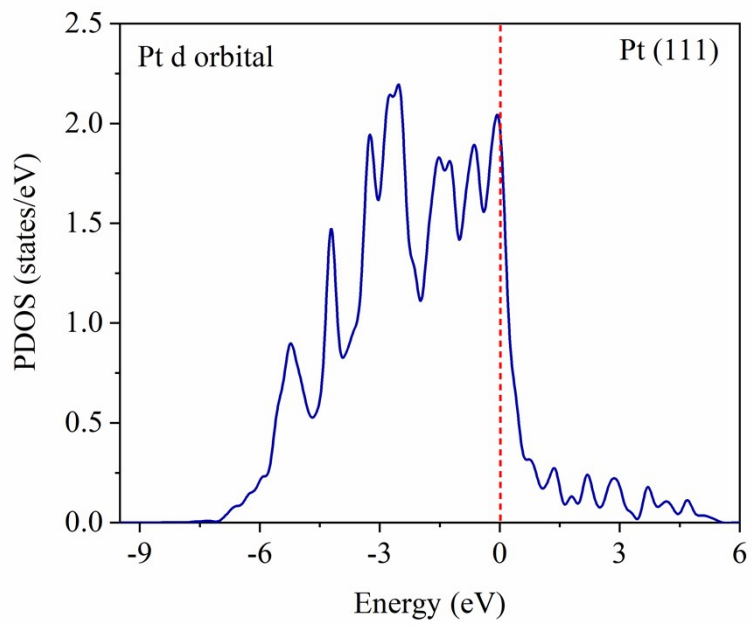
Figure S12. The projected density of states (PDOS) for the Pt-SA/MXene sample.

Table S1. EXAFS fitting parameter for Pt L_3-edge of Pt-SA/MXene.

Sample	Main shell	Atom	N	R (Å)	σ^2 (Å^2)	ΔE_0 (eV)	R factor
	1st	O	2.2±0.5	2.01	0.005	5.8±0.9	0.01
Pt-SA/MXene	2st	Ti	1.1±0.6	2.44	0.01	5.8±0.9	0.01
	3st	Ti	1.7±1.0	2.78	0.01	5.8±0.9	0.01

$S_0^2 = 0.71$, S_0^2 the amplitude reduction factor derived from fitting the Pt foil; N, the coordination number; R, interatomic distance; σ^2, Debye-Waller factor; ΔE_0, edge-energy shift (accounts for the difference between the zero kinetic energy value of the sample and that of the theoretical model). R factor, the goodness of the fitting. The fitting window is from 1.1–3.0 here.

Table S2. The HER activity of the Pt-SA/MXene compared with other recently reported single-atom catalysts in alkaline.

Catalyst	Electrolyte	ICP (wt.%)	Overpotential (mV)	Tafel slopes (mV det^{-1})	Mass loading (mg cm^{-2})	References
Pt-SA/MXene	1.0 KOH	1.01	33	43.9	0.2	This work
Pt$_1$/N-C	1.0 KOH	2.5	46	36.8	0.25	Nat.Commun. 2020, 11, 1029
Ru-NC	1.0 KOH	-	12	24.0	0.2	Nat. Commun. 2019, 10, 631
ECM@Ru	1.0 KOH	0.68	83	59	3.0	Adv. Energy Mater. 2020, 10, 2000882
W-SAC	0.1 KOH	1.21	85	53.0	0.24	Adv. Mater. 2018, 30, 1800396
NiSA-MoS$_2$	1.0 KOH	2.0	98	75	-	Nano Energy 2018, 53, 458
SA-Ru-MoS$_2$	1.0 KOH	5	76.0	21	0.28	Small Methods 2019, 3, 1900653
Ni$_5$P$_4$-Ru	1.0 KOH	3.83	54	52	0.142	Adv. Mater. 2020, 5, 1906972
Pt1/MoO$_{3-x}$/C	1.0 KOH	2	23.3	28.8	0.10	ChemCatChem DOI: 10.1002/cctc.201701777
W-CoP	1.0 KOH	-	40	47.0	-	ACS Sustainable Chem. Eng. 2020, 8,

						14825-14832.
Pt/np-Co$_{0.85}$Se	1.0 KOH	1.03	55	35	2.04	Nat. Commun. 2019, 10, 1743.
Ru-MoS$_2$/CC	1.0 KOH	0.37	41	114	0.23	Appl. Catal. B: Environ. 2019, 249, 91

Table S3. The calculated Bader charge δ over Pt in Pt foil, PtO$_2$ and Pt-SA/MXene in the unit of e. Positive δ means an oxidized state.

Pt-SA/MXene	Pt foil	PtO$_2$
0.17	0.00	1.41